COB09-2539 DEVELOPMENT AND EXPERIMENTAL VALIDATION OF A MATHEMATICAL MODEL FOR ALKALINE MEMBRANE FUEL CELLS (AMFC)

Elise Meister Sommer, elise.sommer@gmail.com
José Viriato Coelho Vargas, jvargas@demec.ufpr.br
Luciana Schmidlin Sanches, lusanches13@hotmail.com
Rafael Bertier Valentim, rafael_bvalentim@hotmail.com
José Eduardo Ferreira da Costa Gardolinski, jegardol@yahoo.com
Universidade Federal do Paraná – UFPR. Bloco IV do Setor de Tecnologia, Centro Politécnico (Campus II), Bairro Jardim das Américas Cx. 19011, CEP 81531-990, Curitiba, PR

Juan Carlos Ordonez, ordonez@eng.fsu.edu
Department of Mechanical Engineering and Cnter for Advanced Power Systems, Florida State University, Tallahasse, Florida 32310-6046, USA

Abstract. *The hydrogen economy is a possible alternative to the current oil based global economy. The technology to build and operate fuel cells is well advanced. However, cost is the reason why fuel cells are not being installed wherever there is a need for more power. Therefore, new conceptions and optimization are a natural alternative to reduce cost and make fuel cells increasingly more attractive for power generation. This paper documents the process of determining the polarization and power curves of the alkaline membrane fuel cell. A general purpose, comprehensive and simplified mathematical model for fuel cells is developed, based on mass, momentum, energy and species conservation, and electrochemical principles. The fuel cell polarization curve, actual power and efficiencies are obtained as functions of temperature, pressure, geometric and operating parameters. Although the model is developed for an alkaline membrane fuel cell (AMFC), it may well be applied to other types of fuel cells, by changing the reaction equations and energy interactions. The parameters used in the mathematical model were obtained for the AMFC prototype by measurements of porosity and permeability, and scanning electron microscopy. Then, the model was experimentally validated through voltage and current measurements performed in the AMFC for different electrolyte concentrations. The model was then adjusted in order to obtain the best value of exchange current density (i0) in the electrodes, which is an important physical property that can be estimated by linearization of the Tafel equation. Since the numerical results showed good qualitative and quantitative agreement when compared to the experimental ones, the value adopted for i0 proved to be appropriate. Another important result of the simulations was the temperature and pressure profiles as functions of the AMFC flow direction.*

Keywords: Mathematical Modeling; Experimental Validation; Alkaline Membrane Fuel Cell.

1. INTRODUCTION

The best way to face the energy crisis, generated by increased demand for energy and by the exhaustion of sources of oil, is to promote a better and more conscious use of the energy resources, combined with the development of renewable sources and their use in accordance with the needs and possibilities of each end user. An attractive alternative is the fuel cell.

The fuel cell is a technology that uses a chemical reaction between oxygen (O_2) and hydrogen (H_2) to generate electricity, releasing as waste heat and water. This concept of energy generation has existed for over 150 years and its development was accelerated in the last 30 years. Fuel cells have recently called attention to the scientific community because its main market of zero pollution electric vehicles. However, to achieve this goal, there are still many obstacles to be overcome. Improvements in the hydrogen storage capacity in the tanks as well as in the durability and power capacity of the fuel cell modules are necessary in order to make the fuel cell powered vehicles commercially viable. It is also necessary to build a system of production and distribution of hydrogen. Therefore, it is extremely necessary a generalized costs reduction.

Fuel cells provide clean energy and with high efficiency in a variety of applications. Moreover, they allow a greater reliability in the energy supply and minimum emission or zero air pollutants. Another advantage of its use, is the ability to co-generate heat because, besides the production of electricity, produces steam.

Among the various types of fuel cells, the alkaline fuel cell (AFC) advantages are high durability and the possibility of using non-noble catalysts, since the kinetics of reduction of oxygen is superior in alkaline media than in acid media. (Burchadt *et al.*, 2002)

Although PEMFC (Polymeric Membrane Fuel Cell) is the most used fuel cell type, to build a polymeric membrane whose efficiency can be compared to the commercial ones remains still a challenge to brazilians researches. Also, the possibility of working with electrodes different than platinum is considered. Platinum short availability and high prices,

and also its unavailability on brazilian soils, determined the choice of a nyquil-cobalt electrode development. As a nyquil-cobalt electrode can not be used in acid media, as in PEMFC's, alkaline media was needed. Thus, to build a completely brazilian alkaline fuel cell, the modified alkaline fuel cell was chosen for this fuel cell development research.

Alkaline Membrane Fuel Cell has an especial differential: its alkaline electrode is not liquid, as on other fuel cell types, but made out of a solid and porous support soaked on a potassium hydroxide solution. Because of this membrane this new type of fuel cell was named AMFC – Alkaline Membrane Fuel Cell. (Figure 1)
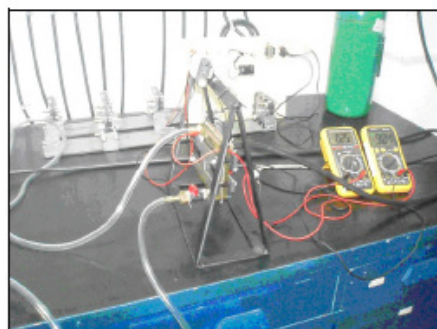

Figure 1 – Alkaline Membrane Fuel Cell (AMFC)

Mathematical modeling and simulation of AMFC allows the knowledge of the influence of important variables (concentration of electrolyte, type of support used and temperature of gases) in its performance.

The goal of this work was to perform the mathematical modeling of alkaline membrane fuel cell (AMFC) and its experimental validation. This will be done by specific goals, that are: adapt the mathematical model of AFC done by Vargas and Bejan (2004) in order to represent the particularities of AMFC; identify the parameters of AMFC, obtain the performance of AMFC as a function of parameters of operation and geometrical, transient, for optimization and control; perform the experimental validation of numerical results; adjust the parameters of the mathematical model for selected cases.

2. MATHEMATICAL MODEL

Vargas and Bejan (2004), developed a mathematical model for an alkaline fuel cell, which was adapted in this study to replace the liquid electrolyte for an alkaline membrane, which is the main feature of the proposed AMFC. In order to mathematically model the AMFC, Volume Element Model was used. (Vargas *et al.*, 2001).

The general idea of the Volume Element Model is to divide the problem domain in smaller volume elements such that the set of volume elements is equal to the original domain. Then, in each volume element, electrochemistry and conservation (mass, energy and species) equations are applied, as well as analytic and empiric literature available correlations, to quantify existent flows. This model adopts for each volume element the classic thermodynamic basic hypothesis of uniform properties in each control volume.

Generally, this local behavior is described with simple functions. The main characteristic of this procedure consists of the use of local approximations on volume elements in which the original domain was divided, instead of using global characteristic approximations.

The developed mathematic model might also be used for other fuel cell types, if the type of electrolyte and reactions are considered using appropriate chemical equations and energetic interactions. (Vargas and Bejan, 2004)

The fuel cell is divided into seven control volumes, which correspond to the most important system parts. They interact energetically with each other and with the environment. These seven control volumes are: CV1 – fuel entrance chamber; CV2 – anode diffusion layer; CV3 – anode reaction layer; CV4 – electrolytic solution and the support; CV5 – cathode reaction layer; CV6 – cathode diffusion layer and CV7 – oxidant entrance chamber.

Modeling considers all present flow phenomena, resulting on a time dependent unidirectional internal flow model with three-dimensional characteristics such as electrolyte wet area and thermal exchange between cell and neighborhoods.

Model algebraic and differential equations solution result on temperature and pressure profile for each control volume on polarization and system potency curves.

Control volumes used on this research were an adaptation of the ones chosen by Vargas and Bejan (2004) and are showed on figure 2.
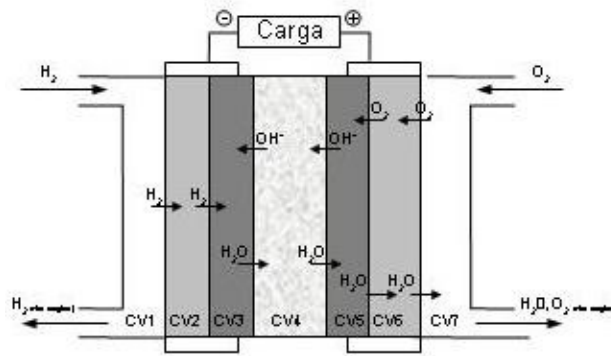
Figure 2. Modeling Control Volumes (Vargas and Bejan, 2004)

Modeling consists on writing conservations equation for each control volume, considering present chemical reactions.

For obtaining real electrochemical potential and consequentially the power, overpotential losses are subtracted from the reversible potential. Losses through kinetic reaction, ohmic losses through electronic and ionic resistance, and concentration losses due to diffusion (mass transportation) are considered as overpotential losses. These losses are cell total current (I) dependent, which is required by external charge (or cell voltage). Analysis was done for transient stage, considering real time control proposal.

Dimensionless variables were defined based on geometry and operational system parameters, i.e. $Pi = p_i/p_\infty$, $\theta i = T_i/T_\infty$, $\tilde{V} = V/V_{ref}$ and $\tilde{I} = I/I_{ref}$.

Resulted equations for the AMFC adopted model used in this research are presented below with brief explanation on the control volume they are related to.

2.1. Fuel and Oxidant entrance chamber (CV1 e CV7)

Fuel enters in the FC in CV1 and then is transported by convection to CV2. The same happens to CV7, but on an opposite way, it is oxygen that enters in CV7 by convection and goes to CV6. CV1 exchanges heat with the environment and with CV2. Besides that there is heat exchange due the hydrogen's transport. For CV7 there's heat exchange with CV6 and environment, and the oxygen transport.

Mass and energy balance for CV1, considering incomprehensive flux, lead to temperature on CV1,

$$\frac{d\theta_1}{d\tau} = \left\{ \frac{N_1}{\psi_f} \left(1 + \tilde{A}_L \xi_1\right)\left(1 - \theta_1\right) + \left(\theta_f - \theta_1\right) + \frac{\tilde{Q}_{12s}}{\psi_f} \right\} \frac{\theta_{1,0}}{P_f} \frac{\gamma_f}{\xi_1} \psi_f \qquad (1)$$

With,

$$\tilde{Q}_i = \dot{Q}_i / (\dot{m}_{ref} c_{p,f} T_\infty) \qquad (2)$$

$$\tilde{Q}_{12} = \tilde{h}_1 \left(1 - \phi_2\right) \left(\theta_2 - \theta_1\right) \text{ where } \tilde{h}_1 = h_1 A_s /(\dot{m}_{ref} c_{p,f}) \qquad (3)$$

Where θ_i is the dimensionless temperature, τ the dimensionless time, ξ_1 the CV length, ψ is the dimensionless mass flow rate, ϕ the porosity, η are the overpotentials and γ the ratio of the species heats (cp/cv). The subscript f means fuel (hydrogen) and ox oxidant, or oxygen in this case.

Mass and energy balance on oxidant entrance space (CV7), incomprehensive non-mixable flux consideration (dm7/dt = 0) and space predominantly fulfilled with dried oxygen consideration lead to:

$$\frac{d\theta_7}{d\tau} = \left[\tilde{Q}_7 + \psi_{ox} \frac{c_{p,ox}}{c_{p,f}} \left(\theta_{ox} - \theta_7\right) + \tilde{H}(\theta_6)_{H_2O} - \tilde{H}(\theta_7)_{H_2O} \right] \frac{R_{ox} \theta_{7,0} \gamma_{ox}}{R_f P_{ox} \xi_7} \qquad (4)$$

2.2 Anode and cathode diffusion layers (CV2 and CV6)

Reactions occur on anodic and cathodic diffusion layers. Both electrodes on a fuel cell are porous to proportionate a large wet superficial area to promote major possible contact between electrolytic solution and electrode and,

consequently, great power density. Porous environment is constituted by one solid and one fluid sides. CV2 fluid mass is negligible if compared to the solid mass. Thus, on energy balance only the solid mass was considered. These control volumes exchange heat with the environment and with neighbors control volumes.

Wet areas on porous anodes and cathodes were estimated by dual-porosity synthesized metal electrodes consideration. Permeability was considered for obtaining each electrode wet area.

Diffusion is considered the dominant mass transport mechanism of gases. Since it occurs in a porous mean, Knudsen flow is used.

Energy and mass balance resulted on the CV2 temperature below:

$$\frac{d\theta_2}{d\tau} = \left[(\theta_1 - \theta_2) + \frac{\tilde{Q}_2}{\psi_f} \right] \frac{\gamma_{s,a} \, \Psi_{H_2}}{\tilde{\rho}_{s,a} (1 - \phi_2) \xi_2} \tag{5}$$

And for CV6,

$$\frac{d\theta_6}{d\tau} = \left[\tilde{Q}_6 + \psi_{O_2} \frac{c_{p,ox}}{c_{p,f}} (\theta_7 - \theta_6) + \tilde{H}(\theta_5)_{H_2O} - \tilde{H}(\theta_6)_{H_2O} \right] \frac{\gamma_{s,c}}{\tilde{\rho}_{s,c} (1 - \phi_6) \xi_6} \tag{6}$$

The oxidant and fuel pressures that enters on catalystic layers are:

$$P_{i,out} = P_{i,in} - \frac{j_i R_i T_\infty L_i \theta_i}{D_i p_\infty}, \quad i = 2, 6 \tag{7}$$

And with $P_{2,in} = P_f$ e $P_{6,in} = P_{ox}$:

$$P_i = \frac{1}{2} \left(P_{i,in} + P_{i,out} \right), \quad i = 2, 6 \tag{8}$$

2.3 Anode and cathode reaction layer (CV3 and CV5)

Reactions take place in these two control volumes. In CV3 electric current is generated and in CV5 it is consumed and OH⁻ generated to replace the ones consumed in the CV3´S reaction, as showed by the equations below:

$$H_{2(g)} + 2OH^-_{(aq)} \rightarrow 2H_2O_{(l)} + 2e^- \tag{9}$$

$$\frac{1}{2}O_{2(g)} + 2H_2O_{(l)} + 2e^- \rightarrow 2OH^-_{(aq)} + H_2O_{(l)} \tag{10}$$

CV3 is divided on 2 compartments, which form the anodic reactional layer: solid and liquid solution. However, on thermal analysis only solid is considered because CV3 fluid mass is negligible if compared to the solid mass. CV3 exchanges heat with neighborhoods and generates heat through ohmic resistance.

CV3 temperature profile becomes:

$$\frac{d\theta_3}{d\tau} = \left[\tilde{Q}_3 - \Delta\tilde{H}_3 + \Delta\tilde{G}_3 \right] \frac{\gamma_{s,a}}{\tilde{\rho}_{s,a} (1 - \phi_3) \xi_3} \tag{11}$$

The reversible electrical potential ($V_{e,a}$) at the anode is given by the Nernst equation,

$$V_{e,a} = V^\circ_{e,a} - \frac{\overline{R} T_3}{nF} \ln Q_3 \tag{12}$$

Where Q is the reaction quotient.

There are two mechanisms for potential losses at the anode: (i) charge transfer (η_{act}), and (ii) mass diffusion ($\eta_{d,a}$). Charge transfer potential loss is obtained from the Butler-Volmer equation for a given current I

$$\frac{I}{A_{3,wet}} = i_{o,a} \left[e^{\frac{(1-\alpha_a)\eta_{act}F}{\overline{R} T_3}} - e^{-\frac{\alpha_a \eta_{act}F}{\overline{R} T_3}} \right] \tag{13}$$

α_a is the anode charge transfer coefficient and $i_{o,a}$ is the anode exchange current density.

Furthermore the mass diffusion potential loss is given by the following equation:

$$\eta_{d,a} = \frac{\overline{R}T_3}{nF} \ln\left(1 - \frac{I}{A_{3,wet}\, i_{Lim,a}}\right) \tag{14}$$

With $i_{Lim,a}$ being limiting current density at the anode that occurs at high values of the surface overpotential

Therefore the resultant electric potential at anode $\left(\tilde{V}_{i,a}\right)$, with dimensionless variables is:

$$\tilde{V}_{i,a} = \tilde{V}_{e,a} - \tilde{\eta}_{act} - \left|\tilde{\eta}_{d,a}\right| \tag{15}$$

Cathode reaction layer (CV5) analysis is analogous to the one presented for the anode reaction layer (CV3).

$$\frac{d\theta_5}{d\tau} = \left[\tilde{Q}_5 - \Delta\tilde{H}_5 + \Delta\tilde{G}_5\right] \frac{\gamma_{s,c}}{\tilde{\rho}_{s,c}\,(1-\phi_5)\xi_5} \tag{16}$$

2.3 Electrolyte (CV4)

Electrolyte in AMFC has a differential them other alkaline fuel cells, it is shaped by the alkaline solution and a porous and inert solid support. For this reason, in energetic and mass balance both solid and liquid parts should be considered. Porosity is the variable used to represent them.

Temperature's profile for CV4 is

$$\frac{d\theta_4}{d\tau} = \left[\tilde{Q}_4 + \tilde{H}(\theta_3)_{H_2O} - \tilde{H}(\theta_4)_{H_2O} + \tilde{H}(\theta_5)_{OH_{aq}^-} - \tilde{H}(\theta_4)_{OH_{aq}^-}\right] \frac{\gamma_{sol}}{\tilde{\rho}_{sol}\,\xi_4} \tag{17}$$

Alkaline solution electrical resistance (R) s given by R4 = L4/(σ As), where σ is the solution electrical conductivity. Hence, there is an ohmic loss in the alkaline solution (CV4). Additionally, potential loss occurs due to electrical resistance of the solution, which penetrates the porous reaction layers in CV3 and CV5. Therefore, the total dimensionless ohmic loss from CV3 to CV5 is

$$\tilde{\eta}_{sol} = \frac{IL_T}{\sigma A_S V_{ref}} \sum_{i=3}^{5} \frac{\xi_i}{\phi_i} \tag{18}$$

3. RESULTS AND DISCUSSION

In this research the behavior of the AMFC was simulated for different conditions. For that it was used a numerical program in FORTRAN to solve the mathematical model's equations. The parameters used in the mathematical model were obtained for the AMFC prototype by measurements of porosity and permeability, and scanning electron microscopy. Then, the model was experimentally validated through voltage and current measurements performed in the AMFC for different electrolyte concentrations. The experimental validation of the mathematical model is performed in detail in this section after the determination of model parameters obtained from experimental procedures. The model was then adjusted in order to obtain the adequate value of exchange current density (i_0) in the electrodes, which is an important physical property that can be estimated by linearization of the Tafel equation.

3.1 Experimental determination of model parameters

In order to obtain the actual physical proprieties of AMFC some lab tests were performed. The aim one was the Scanning Electron Microscopy (SEM) which allows the components structure to be known. SEM's results are shown in figures 3 and 4.

The electrodes used was LT-250-EW, from BASF, with the load of 5g/m² of 30% Pt supported in Vulcan XC-72.

The hydrophilic side of electrode is the one where the alkaline solution penetrates and where the catalyst is deposited, then is where the reactions take place. On SEM pictures can be observed it's structure, typical from composite materials on carbon support. Can be concluded that the use of the electrodes on experimental tests in AMFC didn't damage their structure. The spots that can be viewed should be from KOH crystals. Conversely, about hydrophobic side of electrodes it can be affirmed that is carbon fiber tissues with an ionomer to give the characteristic of hydrophobicity. Neither this side was damaged by the use in tests. From the transverse view the structural difference between the two sides can be observed.
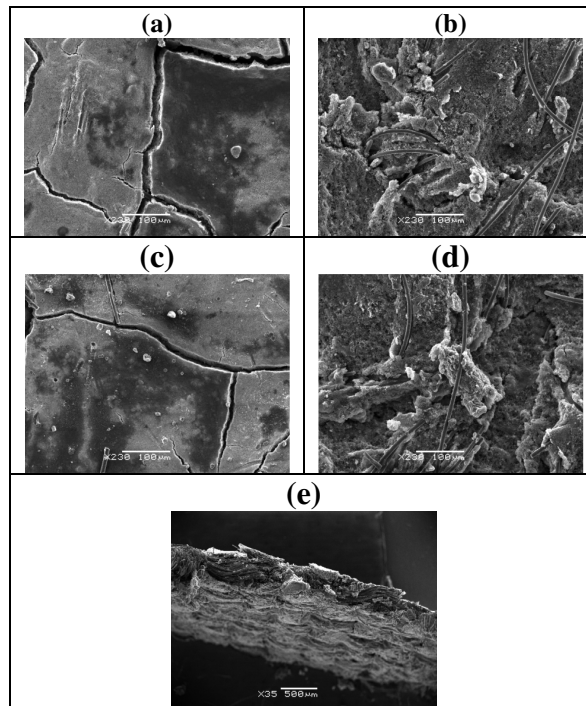
Figure 3. Scanning Electron Microscopy (SEM) of the electrodes used on AMFC. (a) Hydrophilic side of an unused electrode. (b) Hydrophobic side of an unused electrode. (c) Hydrophilic side of an used electrode. (d) Hydrophobic side of an used electrode. (e) Electrode's transverse view.

The solid support's SEM is also shown bellow, were can be observed its high porous structure and affirmed that it well hounded tests in AMFC.
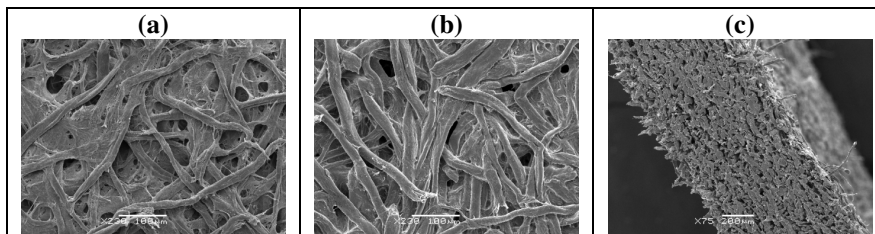

Figure 4. Scanning Electron Microscopy (SEM) of the solid support used on AMFC. (a) Support before be used on AMFC tests. (b) Support after be used on AMFC tests. (c) Support's transverse view.

The others experimental testes resulted in:
- For the alkaline solution the density obtained was 1247 (Kg/m^3);
- The porosity of the solid support was 71%;
- The permeability of the solid support was 4,49s;
- The Heat of Combustion of the electrode was 7255 J and the Higher Heat of Combustion of the solid support was 4320 J.

3.2 Parameters used for the AMFC simulation

The most important parameters used in the simulation are shown in Table 1, as well as the symbols used in the mathematical model. The full list of all parameters used in this research can be found in Sommer (2009).

Table 1 – Parameters used on the AMFC simulation

Symbol	Nomenclature	Unity	Value
α_a and α_c	anode and cathode charge transfer coefficients	-	0,5
$c_{s,a}$ and $c_{s,c}$	anode and cathode specific heat	J kg^{-1} K^{-1}	536,9
H_{fc}	fuel cell height	m	1,0
I_{ref}	reference current	A	1,0
$i_{0,a}$ and $i_{0,c}$	exchange current densities	A m^{-2}	2,169 and 0,217
k_f	fuel thermal conductivity	W m^{-1} K-1	0,0341
k_p	solid suppot thermal conductivity	W m^{-1} K-1	0,1298
$k_{s,a}$ and $k_{s,c}$	anode and cathodethermal conductivity	W m^{-1} K-1	111,78
k_{sol}	solution thermal conductivity	W m^{-1} K-1	0,6071
K_i (i=2,3,5,6)	permeability	m^2	2,5x10^{-13}
$\dot{m}_{ref}$	reference mass flow rate	kg/s	1X10^{-6}
L_T	fuel cell length	m	6,9x10^{-3}
p_∞	external pressure	N m^{-2}	0,1x10^6
R_f	fuel ideal gas constant	J kg^{-1} K^{-1}	4157
R_{ox}	oxidant ideal gas constant	J kg^{-1} K^{-1}	259,8
S_{fc}	fuel Cell thickness	m	8,8x10^{-3}
T_f and T_{ox}	fuel and oxidante temperature	K	298,15
T_∞	external temperature	K	298,15
V_{ref}	reference potential	V	1,0
y	electrolyte solution mass percentage	%	30
$\xi(j)$	dimensionless control volume length	-	0,1 0,333 0,002 0,130 0,002 0,333 0,1
$\rho_{s,a}$ and $\rho_{s,c}$	anode and cathode density	kg m^{-3}	7400
ρ_{sol}	solution density	kg m^{-3}	1247
Φ_i (i=2, 3, 5, 6)	porosity	-	0,038
Φ_4	solid support porosity	-	0,71
σ	electrolyte solution conductivity	ohm^{-1} m^{-1}	40x10^2

3.3 Numerical Results

The numerical simulation was performed by solving Eqs. (1), (4), (5), (6), (11), (16) and (17) in time for obtaining all CV's temperatures and Eqs. (7) and (8) for the gas pressure in CV2 and CV6. Once θ_i and P_i are known the electrical potentials and power are calculated for any assumed current level. Figure 5 shows the electric potential and net power simulated for the AMFC as functions of current.
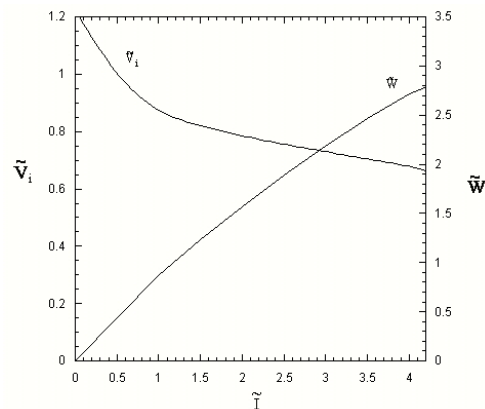

Figure 5. Numerical Power and Polarization Curves

3.3 Parameters adjustment

The model was then adjusted in order to obtain the best value of exchange current density (i_0) in the electrodes, which is an important physical property that can be estimated by linearization of the Tafel equation, when η_{act} is plotted *versus* $\ln i$.

$$\eta_{act} = -\frac{RT}{\alpha nF} \ln i_0 + \frac{RT}{\alpha nF} \ln i \tag{17}$$

When linearized,

$$\eta_{act} = a * \ln i_0 + b * \ln i \tag{18}$$

The values obtained were ($i_{0,a} = 2,169$ e $i_{0,c} = 0,217$). Then the simulation results for these values were compared with the others obtained for values got in literature and usually used. This comparison is shown in figure 6, where the red line represents the experimental results.
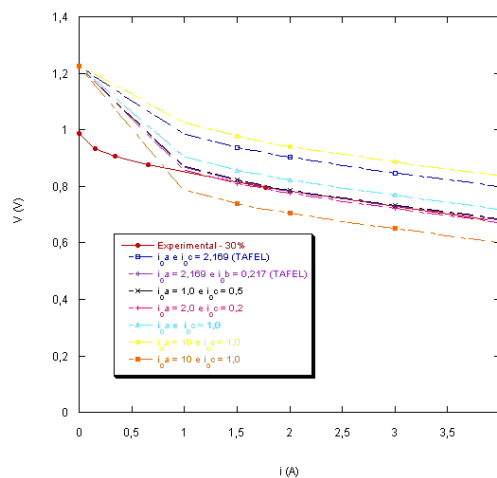

Figure 6.Tests performed to adjust the i0 parameter.

The simulation with the results by linearization of the Tafel equation was the one with nearest results to the experimental ones. .

3.4 Experimental Validation

Numerical curves were then compared with the experimental values obtained on tests performed at AMFC's prototype (Figure 1), for the concentration of electrolyte 30% (mass of KOH by mass of solution), value chosen by have resulted in high values of power experimentally. By the analysis of the experimental uncertainties values (Journal of Heat Transfer. Editorial, 1993) were built bars and rods of errors of twice the standard deviation in experimental values obtained for curves of polarization and power.
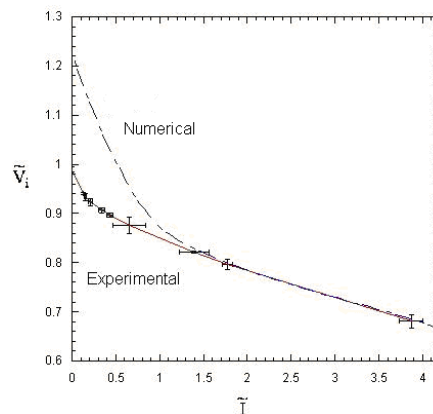

Figure 7. Polarization Curve's Experimental Validation.

The curve of polarization was within the bars of error, only by presenting a shift in low values of current density because the losses from species crossover that occur through the electrolyte, and from internal currents that are not considered in the mathematical model. However fuel cells are expected to operate at the high current densities in order to produce high power and this deviation isn't significant.

The numerical power curve was inside the bar of errors during the current interval analyzed $\left(0 \leq \tilde{I} \leq 4,12 \right)$ and reached the maximum net power value experimentally obtained 2,90 W. (Figure 8)
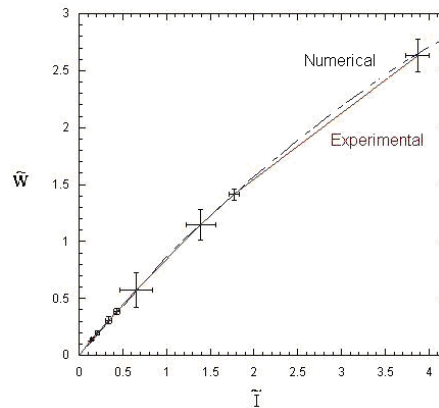

Figure 8. Power Curve's Experimental Validation.

It can be conclude that numerical results showed good concordance both qualitatively and quantitatively with experimental ones.

3.5 Temperature Profile

Others simulations made currently do not usually consider the variation in temperature along the fuel cells. Otherwise it is showed in mathematical modeling that several parameters are affected by temperatures changes, inclusive electrochemical reactions velocity, what will hardly influence on final results of simulation as the potential and electrical power obtained.

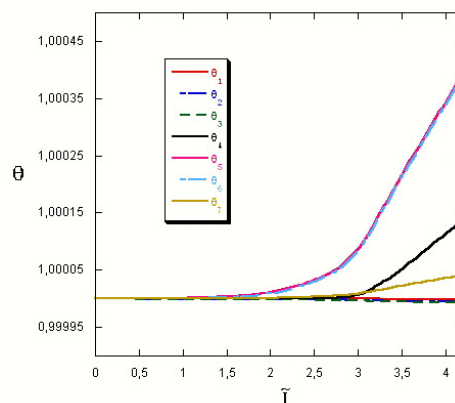Figure 9 shows the temperature profiles obtained for the simulation of AMFC.

Figure 9. The temperature profile of the AMFC.

The variation in temperature resulted from the simulation was small for the current interval evaluated. However, it should be considered, mainly in scale-up of prototype AMFC and in the project of its stack. Furthermore, Martins *et al.* (2009) registered experimentally with a camera infrared temperature variation along a PEMFC. In future this will be done for AMFC and numerical results may be confirmed.

4. CONCLUSIONS

A mathematical model for an Alkaline Membrane Fuel Cell (AMFC) was developed and experimentally validated in this study. The developed model considers the specificities of AMFC, i.e., the electrolyte alkaline membrane. Therefore, the single fuel cell mathematical model to predict fuel cell performance based on operational and geometric parameters was successfully demonstrated.

The parameters used in the mathematical model were obtained for the AMFC prototype by measurements of porosity and permeability, and scanning electron microscopy. Then, the model was experimentally validated through voltage and current measurements performed in the AMFC prototype. Numerical results showed good qualitative and quantitative agreement with the measured experimental data.

The model was then adjusted, through the solution of an inverse problem of parameters estimation for the exchange current density of two electrodes were determined in order to make the numerical as close to possible to experimental. The adequate values were also obtained by Tafel linearization, with good agreement with the numerical procedure, through which the results corroborating theoretically the numerical adjustment.

Another important result of the simulations was the determination of temperature gradients in the flow direction and their dependence on operating current.

The mathematical model developed and experimentally validated in this work could be used in future research as a reliable tool for AMFC simulation, control, design and optimization purposes with low computational time.

5. ACKNOWLEDGEMENTS

Acknowledgements for the Conselho Nacional de Desenvolvimento Científico e Tecnológico - CNPq for the sponsorship of this research. Also, acknowledgments for the Mechanical Engineer Post Graduations Program (PGMEC) of the Universidade Federal do Paraná.

6. REFERENCES

Burchardt, T. et al. Alkaline fuel cells: contemporary advancement and limitations. Fuel, v. 81, p. 2151-2155, 2002.

Journal of Heat Transfer. Editorial, Journal of Heat Transfer policy on reporting uncertainties in experimental measurements and results, ASME, 115, p. 5-6, 1993.

Martions, L. S. et al. The Experimental Validation of a Simplified PEMFC Simulation Model for Design and Optimization Purposes. Applied Thermal Engineering, 2009, submetido a publicação.

Mench, M. M.; Wang, C.; Thynell, S. T. An introduction to Fuel Cells and Related Transport Phenomena. International Journal of Transport Phenomena, v. 3, p. 151-176, 2001.

Sommer, E. M. Desenvolvimento e validação experimental de um modemo matamático de células de combustível alcalinas. Master Degree Dissertation. Mechanical Engineer Post Graduations Program (PGMEC) of the Universidade Federal do Paraná. 2009.

Vargas, J. V. C. et al. A numerical model to predict the thermal and psychometric response of electronic packages. Journal Of Electronic Packaging, Asme, v. 123, p. 200-210, 2001.

Vargas, J.V.C.; Bejan, A. Thermodynamic optimization of internal structure in a fuel cell. International Journal of Energy Research, John Wiley & Sons Ltd, v. 28, p. 319-339, 2004.

Vargas, J. V. C. ; Gardolinski, J. E. F. C.; Ordonez, J. C. Hovsapian, R. ALKALINE MEMBRANE FUEL CELL. Patent, USPTO application number 61/067,404 – 2008.

7. RESPONSIBILITY NOTICE

The authors are the only responsible for the printed material included in this paper.